# Phase-locked regimes in delay-coupled oscillator networks

Nirmal Punetha, Awadhesh Prasad, and Ramakrishna Ramaswamy

Citation: Chaos: An Interdisciplinary Journal of Nonlinear Science **24**, 043111 (2014); doi: 10.1063/1.4897360
View online: http://dx.doi.org/10.1063/1.4897360
View Table of Contents: http://scitation.aip.org/content/aip/journal/chaos/24/4?ver=pdfcov
Published by the AIP Publishing

# Phase-locked regimes in delay-coupled oscillator networks

Nirmal Punetha,[1] Awadhesh Prasad,[1] and Ramakrishna Ramaswamy[2,3]
[1]*Department of Physics and Astrophysics, University of Delhi, Delhi 110007, India*
[2]*School of Physical Sciences, Jawaharlal Nehru University, New Delhi 110067, India*
[3]*University of Hyderabad, Hyderabad 500046, India*

(Received 9 June 2014; accepted 26 September 2014; published online 20 October 2014)

For an ensemble of globally coupled oscillators with time-delayed interactions, an explicit relation for the frequency of synchronized dynamics corresponding to different phase behaviors is obtained. One class of solutions corresponds to globally synchronized in-phase oscillations. The other class of solutions have mixed phases, and these can be either randomly distributed or can be a *splay* state, namely with phases distributed uniformly on a circle. In the strong coupling limit and for larger networks, the in-phase synchronized configuration alone remains. Upon variation of the coupling strength or the size of the system, the frequency can change discontinuously, when there is a transition from one class of solutions to another. This can be from the in-phase state to a mixed-phase state, but can also occur between two in-phase configurations of different frequency. Analytical and numerical results are presented for coupled Landau–Stuart oscillators, while numerical results are shown for Rössler and FitzHugh-Nagumo systems. © *2014 AIP Publishing LLC*.
[http://dx.doi.org/10.1063/1.4897360]

**Time-delay couplings are ubiquitous in natural systems and typically arise due to the finite speed of signal propagation between the interacting units. Such coupling can cause the system to exhibit dynamics that are not observed for instantaneous coupling, namely for zero time-delay. In this work, we study the nature of phase synchronization in a system of globally delay-coupled oscillators as a function of the coupling parameters and system size. When the time-delay is varied there can be, depending on the system size and the coupling strength, a discontinuous change in the phase and frequency response of the system which can go from a synchronous in-phase state to a mixed-phase synchronous state. There can also be transitions between two in-phase states with different frequencies. These transitions are observed in the regime of sustained oscillations and also in the transient dynamics of the amplitude-death region. For the former case, we carry out a stability analysis of the synchronized solutions, while for the latter, the change in phase behavior can be tracked through eigenvalue analysis of the Jacobian matrix at the fixed point.**

## I. INTRODUCTION

Ensembles of globally coupled oscillators are abundant in nature, and they frequently exhibit collective behavior. Well known examples include the synchronization of flashing-fireflies,[1] clapping of large audiences,[2] lasers arrays,[3] chemical,[4,5] and biological oscillators,[6–9] When the speed of information transfer in such settings is finite, then the coupling between the various subunits involves time-delay. This can significantly influence the system dynamics:[10–12] a number of effects that are modified as a result of delay-coupling, including aspects of synchronization,[13–16] amplitude death,[17,18] phase-flip,[19,20] multistability, and hysteresis.

In an ensemble of coupled oscillators, within the synchronized regime, there can be different states characterized by the nature of the individual oscillator phases (see the schematic in Figs. 1(a) and 1(b) for two and three oscillators). All the elements can be oscillating in-phase and in

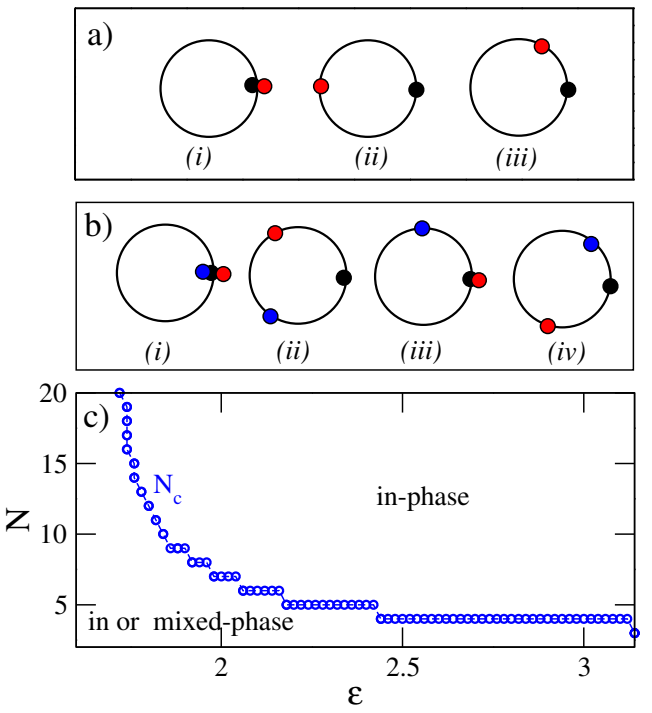


FIG. 1. Schematic depiction of the phase relationship of (a) two and (b) three phase oscillators. In both (a) and (b), configurations (i) in-phase and (ii) splay-phase are stable solutions that can be achieved for all parameter values, while the arbitrary phase configurations [(iii) and (iv)] depend upon coupling parameters. (c) Summary of results as a function of $N$ and $\varepsilon$: Beyond a critical value $N_c(\varepsilon)$, mixed phase solutions are not stable (see the text for details).

 

perfect synchrony for instance (Figs. 1(ai) and 1(bi)). A second state is the so-called splay-phase:[21] the phases of the oscillators are equally spaced on the circle (Figs. 1 (aii) and 1(bii)). Such states have been observed in the absence of delay[21,22] as well as in delay coupled oscillators.[23–25] In addition, one can also observe the phase-locked solutions with arbitrary-phase differences (Figs. 1(aiii), 1(biii), and 1(biv)). The later two states are termed *mixed*;[26] such states have been observed in neuronal models,[27] as well as experimentally in coupled chemical,[24] and optoelectronic oscillators.[25]

The various stable phase configurations that can result in a complex system represent distinct activity patterns within the synchronized regime,[28,29] and the study of such states has therefore attracted considerable interest. In addition, there is the question of bifurcations and transitions between different phase states. One transition that has been studied in some detail is the phase-flip,[19] a transition from the purely in-phase state to an anti-phase state, accompanied by a frequency jump.[30,31] In recent work,[23–25] the distinct phase behavior of a network of oscillators arranged in a ring has been studied in detail. Interesting questions relating to the emergence of such states for different connection topologies and the effect of system size still need to be explored.

In this paper, we study the effect of varying system size in an ensemble of globally coupled oscillators. For low coupling strength, both in-phase or splay solutions can exist for finite system size (see Fig. 1(c)), but for strong coupling and larger networks, the splay-phase states disappear. Thus, when the coupling parameters are varied, there can be a transition either from in-phase to in-phase motion, or from splay-phase dynamics to in-phase motion. The system remains synchronized through the transitions; with increasing system size, the frequencies of the mixed-phase state are affected while that for in-phase motion remains unchanged. We obtain a general relation to estimate these frequencies in an ensemble of globally delay-coupled oscillators and discuss the nature of possible transitions in the system through stability analysis.

In Sec. II, we consider an ensemble of delay coupled oscillators and analytically estimate the synchronized frequencies and phase solutions of the system. We discuss the effect of system size variation on the frequencies and phases and present numerical results in Sec. III. The stability analysis of the synchronized state as a function of network size is presented in Sec. IV A; eigenvalue analysis is presented in Sec. IV B. This makes it possible to derive limited analytic results in the present situation. Numerical results for coupled Rössler and FitzHugh-Nagumo model are presented in Sec. V, suggesting that these results may have wide applicability in other complex dynamical systems. The paper concludes with a brief discussion and summary in Sec. VI.

## II. PHASE LOCKED SOLUTIONS

The equations of motion for an ensemble of $N$ globally coupled Landau-Stuart oscillators with time-delayed interactions are

$$\dot{Z}_j = \left(1 + i\omega_j - |Z_j|^2\right)Z_j + \frac{\varepsilon}{(N-1)}\sum_{k\neq j}\left(Z_k(t-\tau) - Z_j(t)\right), \tag{1}$$

where $Z_j$ is the complex amplitude of the $j^{th}$ oscillator, $\omega_j$ its intrinsic frequency, the coupling strength is $\varepsilon$, and $j$, $k = 1, 2, \ldots, N$.

Numerical studies of the phase behavior of Eq. (1) as a function of the coupling parameter $\varepsilon$ and system size $N$ are summarized in Fig. 1(c). For lower coupling strengths and smaller networks, we find an interval in the time-delay when the system can show mixed-phase behavior. When the time delay is varied, the system abruptly jumps from in-phase motion to mixed-phase dynamics and then reverts to in-phase dynamics. For higher couplings, this window decreases with increasing network size, and disappears after a critical system size $N_c(\varepsilon)$. It is to be noted that these transitions are observed not only in oscillatory regime, but also in the transient dynamics of amplitude death region where the system eventually goes to a fixed point.

It is possible to obtain an analytic estimation of the synchronized frequencies of the system in the weak coupling limit. Making the approximation that amplitude variations of the system can be ignored, and one can focus upon the phase dynamics, then for identical or nearly identical oscillators, the dynamics of the corresponding phase variables reduce to that of the Kuramoto model,[4] given as[30,31]

$$\dot{\phi}_i = \omega + \frac{\varepsilon}{(N-1)}\sum_{j\neq i}\sin\left(\phi_j(t-\tau) - \phi_i(t)\right), \tag{2}$$

where $\phi_i$ is the phase of $i^{th}$ oscillator. In the synchronized regime, the oscillators move with the same common frequency $\Omega$, and the solutions can be written in terms of $\Omega$ and constant phases $\alpha_i$ as

$$\phi_i(t) = \Omega t + \alpha_i, \quad i = 1, 2, \ldots, N. \tag{3}$$

If we consider $\alpha_1 = 0$ as a reference angle, then $\alpha_j$, $j = 2, 3, \ldots, N$ will be the phase difference of the $j^{th}$ oscillator with respect to the first one. It is straightforward to see that the relation between collective frequency $\Omega$ and constant phases $\alpha_i$ is

$$\Omega = \omega - \frac{\varepsilon}{(N-1)}G_i, \tag{4}$$

where

$$G_i = \sum_{j\neq i}\sin\left(\Omega\tau - (\alpha_j - \alpha_i)\right), \quad i,j = 1, 2\ldots N. \tag{5}$$

Averaging Eq. (4) over all oscillators gives

$$\Omega = \omega - \frac{\varepsilon}{N(N-1)}G, \tag{6}$$

where

$$G = \sum_{i=1}^{N} G_i = \sum_{i=1}^{N}\left(\sum_{j\neq i}\sin\left(\Omega\tau - (\alpha_j - \alpha_i)\right)\right).$$

On further simplification, this reduces to

$$G = \sum_{i=1}^{N}\left(\sin(\Omega\tau)\sum_{j\neq i}\cos(\alpha_j-\alpha_i)\right) - \sum_{i=1}^{N}\left(\cos(\Omega\tau)\sum_{j\neq i}\sin(\alpha_j-\alpha_i)\right). \quad (7)$$

The second term vanishes, and the first gives

$$G = 2\sin(\Omega\tau)\sum_{i,j>i}\cos(\alpha_j-\alpha_i), \quad (8)$$

so that Eq. (6) can be rewritten as

$$\Omega = \omega - \frac{2\varepsilon\sin(\Omega\tau)}{N(N-1)}\left(\sum_{i,j>i}\cos(\alpha_j-\alpha_i)\right). \quad (9)$$

If one defines $\alpha_{kl}=\alpha_k-\alpha_l$, and the quantity

$$\tilde{c} = \frac{\sum_{i,j>i}\cos(\alpha_j-\alpha_i)}{N(N-1)/2} = \langle\cos(\alpha_{ij})\rangle, \quad (10)$$

namely, the averaged cosine of phase differences for all oscillator pairs, it becomes possible to rewrite Eq. (9) for the the synchronized collective frequency in compact form as

$$\Omega = \omega - \varepsilon\tilde{c}\,\sin(\Omega\tau), \quad (11)$$

where $|\tilde{c}|\leq 1$. This general transcendental relation gives the frequency of synchronized motion for $N$ globally delay-coupled oscillators.

The condition for synchronization, from Eq. (4), is

$$G_1 = G_2 = \cdots = G_N,$$
$$\text{i.e., } \sum_{j\neq 1}\sin(\Omega\tau-\alpha_{j1}) = \sum_{j\neq 2}\sin(\Omega\tau-\alpha_{j2}) = \cdots = \sum_{j\neq N}\sin(\Omega\tau-\alpha_{jN}). \quad (12)$$

Solutions for $\alpha$'s from Eq. (12) provide possible phase configurations. This information can then be used in Eqs. (10) and (11) to calculate the $\tilde{c}$ and the synchronized frequencies respectively.

It can be seen that there are two trivial ways in which the synchronization condition Eq. (12) can be satisfied. For the *in-phase* solution, all $\alpha_{ij}=0$ and hence $\tilde{c}=1$. This case has been extensively studied.[16] The other case is the *splay* state with all phases equally spaced, namely

$$\alpha_j = (j-1)\frac{2\pi}{N}; \quad j=1,2,\ldots,N. \quad (13)$$

This solution can occur for arbitrary $\tau$ and $\Omega(\tau)$ and has $\tilde{c}\neq 1$. The splay configuration for two oscillators is the anti-phase state; this is known to occur with delay coupling and has been examined in detail in the context of the phase-flip transition[30,31]

Depending upon the values of $\tau$ and $\Omega(\tau)$, there may be other mixed-phase configurations satisfying Eq. (12). Although finding these solutions analytically by solving Eqs. (11) and (12) is nontrivial, we encounter such phase states in numerical simulations.

## III. SYSTEM-SIZE EFFECTS

Here, we analyze the effects of coupling parameters and size of the network on synchronized frequencies $\Omega$ and corresponding phase behaviors. It is clear that the value of $\tilde{c}$ in Eq. (10) will depend upon how the $\alpha$'s are distributed. Possible distributions for two and three oscillators are illustrated below.

(i) $N=2$: For arbitrary $\alpha_i$, the synchronization condition $G_1=G_2$ gives the relation $\sin\bar{\alpha}\cos\Omega\tau=0$, where $\bar{\alpha}=\alpha_1-\alpha_2$. If $\sin\bar{\alpha}=0$, then both in-phase and out-of-phase (in this case, this is the splay) solutions are possible for arbitrary values of $\tau$ and $\Omega(\tau)$, as shown in Figs. 1(ai) and 1(aii), respectively. However, if $\cos\Omega\tau=0$ (i.e., $\Omega\tau=\pi/2,\ 3\pi/2,\ldots$) then the synchronized solutions can have an arbitrary phase difference $\bar{\alpha}$, which depends upon initial conditions (Fig. 1(aiii)).

(ii) $N=3$: Although finding a compact analytical condition for synchronization by setting $G_1=G_2=G_3$ is nontrivial, synchronized solutions do exist for $\alpha_i=0$ (in-phase, Fig. 1(bi)) and for $\min\{|\alpha_i-\alpha_j|, 2\pi-|\alpha_i-\alpha_j|\}=2\pi/3$ (splay phase, Fig. 1(bii)). An arbitrary phase configuration say $\alpha_1=\alpha_2=\alpha$ demands, from the synchronization condition, $\tan\Omega\tau=3\sin(\alpha_3-\alpha)/(1-\cos(\alpha_3-\alpha))$, and clearly depends on $\tau$ and $\Omega(\tau)$. Such arbitrary phase configurations are possible only for certain values of $\tau$, $\Omega(\tau)$; see Figs. 1(biii) and 1(biv).

We examine the behavior of synchronized frequencies and corresponding phase configurations as a function of the delay for arbitrary system sizes $N$. The variation of $\langle\tilde{c}\rangle$ as a function of $N$ in Eq. (1) is shown in Fig. 2(a), the average $\langle\cdot\rangle$ being taken over $10^3$ initial conditions. The different curves correspond to different values of coupling strengths for fixed time-delay $\tau=\pi/\omega$. $\tilde{c}$ is calculated numerically[32] from the phases $\alpha_i=\tan^{-1}(\mathrm{Im}\,Z_i/\mathrm{Re}\,Z_i)$ of the oscillators in Eq. (1). As can be clearly seen there are two curves $C_1$ and $C_2$: the first corresponding to the in-phase solution, $\tilde{c}=1$, while the second is a mixed-phase solution with $\tilde{c}\neq 1$. The leading behaviour as a function of $N$ appears to be $\tilde{c}\propto -(N-1)^{-1}$.[33]

The fluctuations in $\tilde{c}$ decrease with $N$; shown in Figs. 2(b) and 2(c) are the distributions of $\tilde{c}$ for $N=6$ and 15 for the mixed phase case. The variance decreases with increasing number of oscillators, and $\tilde{c}\to 0$ indicating effectively uncoupled behavior when $\omega=\Omega$. Similar variations in $\langle\tilde{c}\rangle$ are observed for different values of delays for fixed coupling strengths since $\tilde{c}$ in Eq. (10) does not explicitly depend upon coupling parameters $\varepsilon$ or $\tau$ (data not shown here).

In Fig. 3, we numerically illustrate the transitions between different phase states when the parameters are varied, and the effect of network size on these transitions. The variation of $\tilde{c}$ and the synchronization frequency, calculated numerically, is shown as a function of the delay parameter $\tau$ in Figs. 3(a) and 3(b), respectively. The coupling strength is fixed, $\varepsilon=2$, and the number of oscillators is varied. There

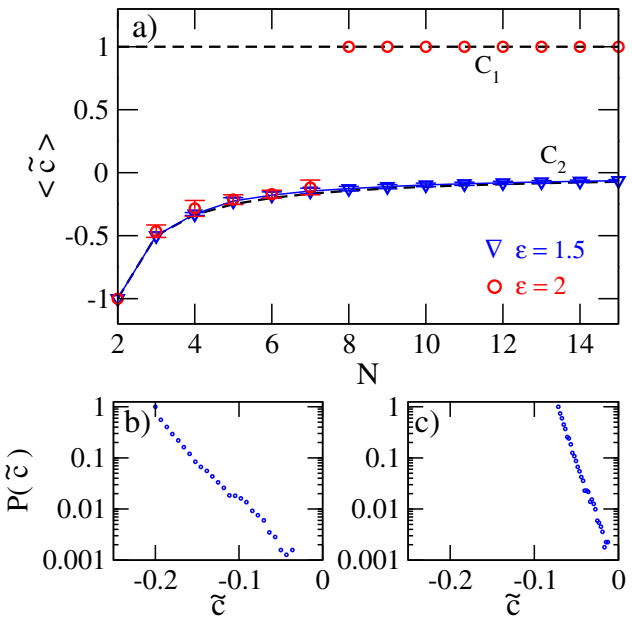


FIG. 2. (a) The variation of $\tilde{c}$ as a function of $N$ at $\tau = \pi/\omega$ ($\omega = 5.0$). The analytical curves $C_1$ and $C_2$ (dashed lines) represent in-phase ($\tilde{c} = 1$) and mixed-phase (Eq. (11)) solutions respectively. Symbols ○ and △ correspond to the numerically calculated values of $\tilde{c}$ from Eq. (1). Errors bars in (a) correspond to the standard deviation in $\tilde{c}$, calculated from $10^3$ initial conditions. The distributions of $\tilde{c}$ calculated from $10^4$ initial conditions for (b) $N = 6$ and (c) $N = 15$ at $\varepsilon = 1.5$.

are windows in delay parameter (when $\tilde{c} \neq 1$), wherein the system has the mixed-phase configurations. These also suggest that different types of phase relations can be found at the same delay for different $N$, e.g., at $\tau = 0.6$ there are out-of-phase, mixed-phase and in-phase solutions for $N = 2$, 6, and 8, respectively. For a small number of oscillators, say

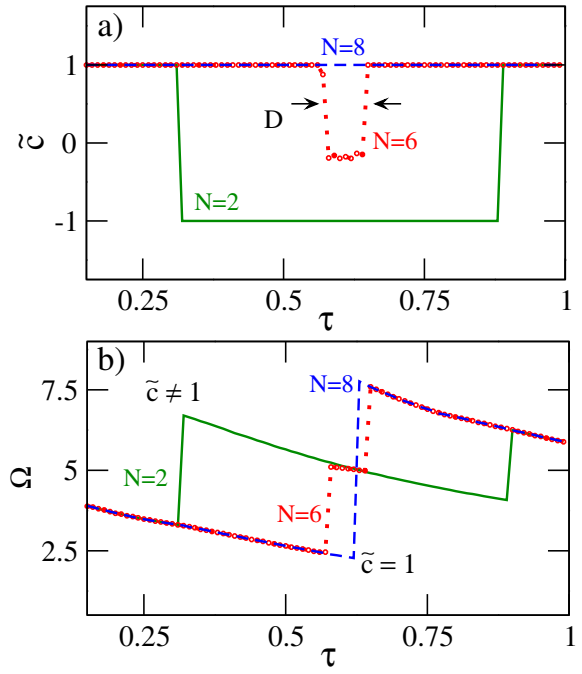


FIG. 3. The variation of (a) $\tilde{c}$ and (b) common frequency for the system, Eq. (1), as function of time-delay $\tau$ for different number of oscillators $N = 2$ (solid-green line), 6 (dotted-red line) and 8 (dashed-blue line).

$N = 2$ and 6, when the delay is increased, the frequency of in-phase motion when $\tilde{c} = 1$ decreases and then jumps to higher value having mixed-phase, $\tilde{c} \neq 1$. On further increase of delay, the frequency again jumps to another higher value with in-phase motion (namely $\tilde{c} = 1$).

For more oscillators, say above $N = 8$ (see Figs. 3(a) and 3(b)), the intermediate mixed-phase does not appear and the motion goes from in-phase to in-phase dynamics. This is also evident from Fig. 2, where the solution switches from mixed-phase (curve $C_2$) to in-phase ($C_1$) when the number of oscillators is increased at fixed coupling parameters: for example, when $\varepsilon = 2$, there is switching from mixed-phase to in-phase at $N = 8$.[34]

As we see in Fig. 3 that the width of the splay window, represented by $D$, decreases with the increase of number of oscillators, its variation with $N$ is shown in Fig. 4 for different coupling strengths $\varepsilon$. For weak coupling (e.g., $\varepsilon = 0.25$ and 1.5), the curve flattens, and hence, there is always a possibility of the mixed-phase solution even for a large number of oscillators, but for strong coupling (say $\varepsilon = 2$ or higher), this width decreases to zero at specific $N = N_c(\varepsilon)$, and hence, only in-phase solutions can exist thereafter.

## IV. FREQUENCY TRANSITIONS

Depending upon the parameter values and system size, the system makes an abrupt transition from in-phase motion (curve $C_1$) to mixed-phase dynamics ($C_2$) with an abrupt change in frequency as well (Fig. 3). These transitions occur both in the regime of oscillatory motion as well as in the transient dynamics of the amplitude death region. In the former case, the transitions can be explained by analyzing the stability of the synchronized solutions ($\Omega t + \alpha_i$, $i = 1\ldots, N$), and in the latter, by an eigenvalue analysis around the stable fixed point. We discuss these below.

### A. Oscillatory regime: Stability of splay solutions

The Master Stability Function (MSF) approach[35–37] is a general framework to detect the stability of synchronized solutions in a network of oscillators. Using this approach, one can separate the local dynamics of individual oscillator from the network topology given by the adjacency matrix. The analytical

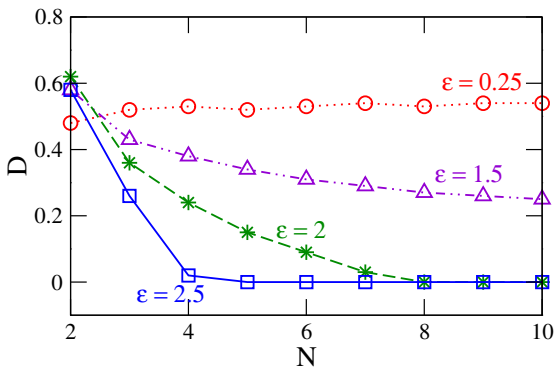


FIG. 4. The variation of width $D$, the window corresponding to the mixed-phase solution, as a function of number of oscillators at different values of coupling strengths.

expression for stable synchrony is obtained by diagonalizing the variational equation for synchronized states. This is achieved by either considering the case of in-phase states for all networks or by taking splay states in special networks[23,24]—unidirectional ring, for example. However, implementation of MSF approach to find the stability of splay states is limited for some networks such as globally coupled oscillators (as considered in this work). Therefore, in this case, we numerically examine the dynamics of perturbations from the synchronized states. We consider small perturbations $\xi_i$ from the splay synchronized solutions, i.e., $\phi_i(t) = \Omega t + \alpha_i + \xi_i$, where $\alpha_i = (i-1)\frac{2\pi}{N}$, $i = 1, 2, \ldots, N$ (cf. Eq. (13)). Plugging these solutions in Eq. (2) we get

$$\Omega + \dot{\xi}_i = \omega + \frac{\varepsilon}{(N-1)} \sum_{j \neq i} \sin\left[-\Omega\tau + \alpha_{ji} + \xi_j(t-\tau) - \xi_i(t)\right], \tag{14}$$

where $\alpha_{ji} = \alpha_j - \alpha_i$. Expansion of this equation upto the first order gives

$$\Omega + \dot{\xi}_i = \omega + \frac{\varepsilon}{(N-1)} \sum_{j \neq i} \sin\left(-\Omega\tau + \alpha_{ji}\right) + \frac{\varepsilon}{(N-1)} \sum_{j \neq i} \cos\left(-\Omega\tau + \alpha_{ji}\right)\left[\xi_j(t-\tau) - \xi_i(t)\right]. \tag{15}$$

Splay configurations, $\phi_i(t) = \Omega t + \alpha_i$, are the solutions of Eq. (2), therefore the variational equation can be written as

$$\dot{\xi}_i = \frac{\varepsilon}{(N-1)} \sum_{j \neq i} \cos\left(-\Omega\tau + \alpha_{ji}\right)\left[\xi_j(t-\tau) - \xi_i(t)\right]. \tag{16}$$

These perturbations must die out for stable synchronized states. Since the coefficients of the variables $\xi_i$ are not constant,[38] it is nontrivial to obtain a stability criterion by solving these equations analytically. However, to detect the behavior of the perturbations, we numerically[32] calculate the Lyapunov exponents of the system Eq. (16) (not shown here). Note that one of the Lyapunov exponent of the system Eq. (16) is always zero corresponding to the perturbations on the synchronization manifold. A positive largest Lyapunov exponent indicates the instability of splay-phase synchronization states. In case the largest Lyapunov exponent is zero, the second largest exponent determines the nature of dynamics: its zero and negative values correspond to the neutrally stable and stable splay synchronization states respectively.

Shown in Fig. 5 are the stability regions for splay states in $(\Omega - \tau)$ plane for different values of $N$ at $\varepsilon = 2$. This figure shows that the stable splay states (blue regions) only exist for $N = 2$ and 3. However, for $N > 3$, the splay states are at best neutrally stable (green regions), which too disappear as the number of oscillators in the network (cf. $N = 4$, 8 in Figs. 5(c) and 5(d)) are increased.

The stability criterion for in-phase solutions is independent of number of oscillators and given by $\varepsilon\cos(\Omega\tau) > 0$[16] as can be seen from Eq. (16) with all $\alpha_{ji} = 0$. This suggests that when the size of the network $N$ increases, the system can only exhibit in-phase behavior since the stable regions for splay states either become neutrally stable, or even unstable, while the stability of in-phase solutions remain unaffected. This stability analysis confirms the absence of splay states in sufficiently large systems for high coupling strengths, as shown in Fig. 1(c).

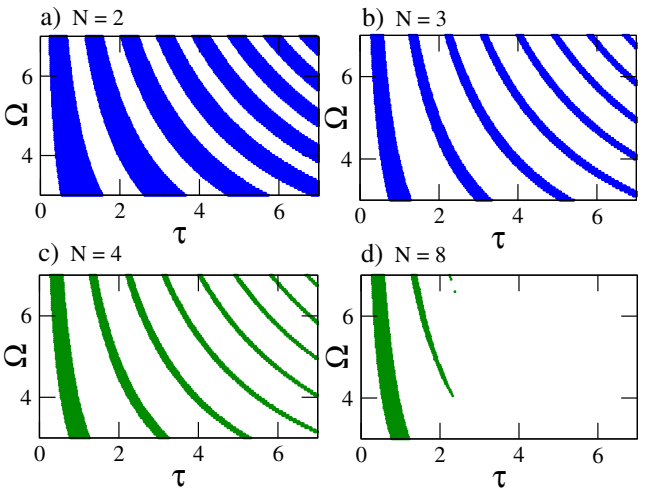


FIG. 5. The stability diagram for the splay states for (a) $N = 2$, (b) $N = 3$, (c) $N = 4$, and $N = 8$ oscillators in $(\Omega - \tau)$ plane. Shaded blue (or green) and blank (white) regions correspond to the stable (or neutrally stable) and unstable splay states, respectively. The stability is determined by calculating Lyapunov exponents of Eq. (16) numerically. Shaded regions in (a) and (b) correspond to the stable, while in (c) and (d), represent neutrally stable splay states.

### B. Amplitude death region: Eigenvalue crossings

In this subsection, we analyze the frequency transitions within the amplitude death region. An analytical study of the transient dynamics is possible since the system asymptotically approaches a fixed point, in this case the origin. The frequency of the damped motion is given by the imaginary part of the leading eigenvalue of the Jacobian at the fixed point, while the real part of the eigenvalue is simply the largest Lyapunov exponent.

The frequency transitions occur at parameter values where the real parts of the eigenvalues cross each other.[30,31] Assuming an exponential time-dependence of perturbations, namely $\delta y(t) \propto \exp(\lambda t)$, the Jacobian (at the origin) for $N$ coupled identical Landau–Stuart oscillators is (with $\mu = 1 + i\omega - \varepsilon$ and $\gamma = \varepsilon e^{-\lambda\tau}/(N-1)$)

$$\mathbf{J} = \begin{pmatrix} \mu & \gamma & \cdots & \gamma \\ \gamma & \mu & \cdots & \vdots \\ \vdots & \vdots & \vdots & \vdots \\ \vdots & \cdots & \mu & \gamma \\ \gamma & \cdots & \cdots & \mu \end{pmatrix}. \tag{17}$$

This is a symmetric matrix with eigenvalues

$$\begin{pmatrix} \lambda_1 \\ \lambda_2 \\ \lambda_3 \\ \vdots \\ \lambda_N \end{pmatrix} = \begin{pmatrix} \mu + (N-1)\gamma \\ (\mu - \gamma) \\ (\mu - \gamma) \\ \vdots \\ (\mu - \gamma) \end{pmatrix}, \tag{18}$$

namely,

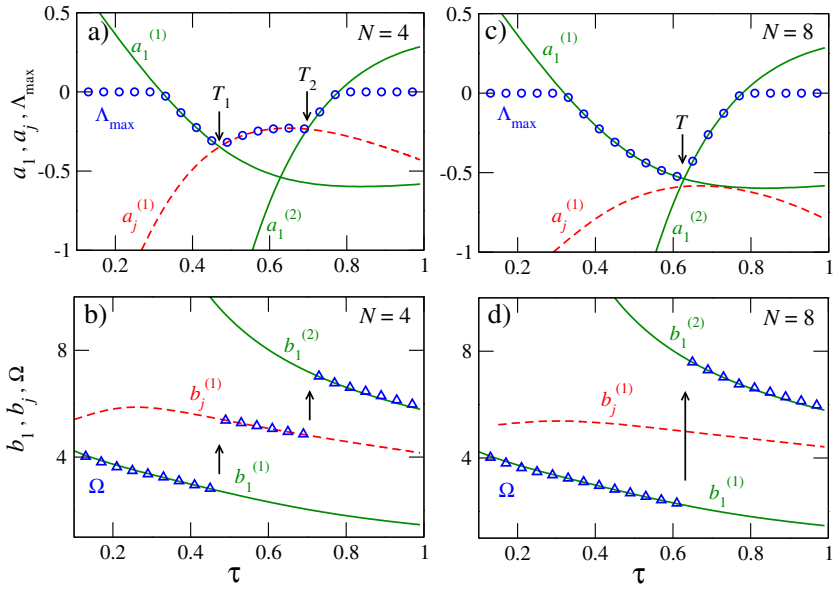


FIG. 6. The variation of real part $a$'s of the eigenvalues for system size $N=4$ and $N=8$ is plotted with time-delay $\tau$ in (a) and (c), respectively. Corresponding imaginary parts $b$'s are plotted in (b) and (d). The variation of largest Lyapunov exponent $\Lambda_{max}$ and numerically calculated frequencies $\Omega$ of the system (Eq. (1)) with time-delay is plotted by blue circles and triangles, respectively. The system parameters are $\omega=5$, $\varepsilon=2$.

$$\lambda_1 = 1 + i\omega - \varepsilon + \varepsilon\exp(-\lambda_1\tau) \tag{19}$$

and

$$\lambda_j = 1 + i\omega - \varepsilon - \frac{\varepsilon}{(N-1)}\exp(-\lambda_j\tau); \quad j = 2, 3, \ldots, N. \tag{20}$$

Taking $\lambda_i = a_i + ib_i$, and separating real and imaginary parts, from Eq. (19), one gets

$$\begin{aligned} a_1 &= 1 - \varepsilon + \varepsilon\exp(-a_1\tau)\cos(b_1\tau), \\ b_1 &= \omega - \varepsilon\exp(-a_1\tau)\sin(b_1\tau), \end{aligned} \tag{21}$$

which have no $N$ dependence. The other eigenvalues, $\lambda_j = a_j + ib_j$ given by Eq. (20), however, depend upon $N$; their real and imaginary parts are

$$\begin{aligned} a_j &= 1 - \varepsilon - \frac{\varepsilon}{(N-1)}\exp(-a_j\tau)\cos(b_j\tau), \\ b_j &= \omega + \frac{\varepsilon}{(N-1)}\exp(-a_j\tau)\sin(b_j\tau). \end{aligned} \tag{22}$$

For $N>2$, it is only possible to solve Eqs. (21) and (22) numerically.

Shown in Fig. 6 are the variations of $a_1$, $a_j$ (top row) and $b_1$, $b_j$ (bottom row) for $N=4$ (left panel) and 8 (right panel) as a function of time-delay, the solid and dashed lines corresponding to solutions of Eqs. (21) and (22) respectively. There can be multiple solutions to Eqs. (21) and (22), and these are identified by superscripts, $a_i^{(k)}$ and $b_i^{(k)}$. Computed values of the largest Lyapunov exponent[32] $\Lambda_{max}$ (circles) and frequencies $\Omega$ (triangles) of the system (Eq. (1)) are also shown.

Solutions to Eq. (21) corresponding to in-phase motion are unaffected by the system size, unlike the roots of Eq. (22) which correspond to mixed-phases. In Fig. 6(a) the real part of the eigenvalue $a_j^{(1)}$ crosses the leading eigenvalue $a_1^{(1)}$ at the point $T_1$. Since the frequency of the system is given by the imaginary part of the leading eigenvalue, the system jumps into the corresponding frequency $b_j^{(1)}$ at this crossing as shown in Fig. 6(b). With further increase in delay, we see another such crossing at $T_2$ between $a_j^{(1)}$ and $a_1^{(2)}$, leading to an another frequency jump into an in-phase frequency $b_1^{(2)}$. Unlike $a_1$ and $b_1$, the variation of $a_j$ and $b_j$ with delay changes with system size. We see the consequence of the $N$-dependence of eigenvalues in Fig. 6(c), where for $N=8$, $a_j^{(1)}$ now does not cross the largest eigenvalue. Instead, here, two roots of $N$-independent eigenvalues $a_1^{(1)}$ and $a_1^{(2)}$ cross at $T$. Therefore, in this case, we observe the corresponding jump from one in-phase $b_1^{(1)}$ to another in-phase frequency $b_1^{(2)}$ (cf. Fig. 6(d)).

The above analysis in the amplitude death region shows that whenever there is a crossing between the leading eigenvalue and another, there *must* be a dynamical transition with a frequency discontinuity. These can either be from in-phase to mixed-phase or even between two in-phase frequencies, depending on the specific eigenvalues involved in the crossings. When $a_1^{(k)}$ crosses $a_j^{(k)}$, the transition occurs between in-phase and mixed-phase states, but when the crossing is between two different roots of $a_1$, then the transition is from in-phase to in-phase motion.

## V. OTHER MODEL SYSTEMS

Under certain conditions, the phase dynamics of several systems can be approximated by the Kuramoto model.[4] One may therefore anticipate that the results obtained above will apply to a wider class of model oscillators. Here, we present a numerical study of coupled Rössler oscillators as well as coupled FitzHugh-Nagumo (FHN) neuronal model systems.

First consider globally coupled Rössler oscillators for which the equations of motion are given by (time-delay is included in the coupling)

$$\begin{aligned} \dot{x}_i &= -\omega_i y_i - z_i + \frac{\varepsilon}{(N-1)}\sum_{j\neq i}\big(x_j(t-\tau) - x_i(t)\big), \\ \dot{y}_i &= \omega_i x_i + a y, \\ \dot{z}_i &= f + z(x-c). \end{aligned} \tag{23}$$

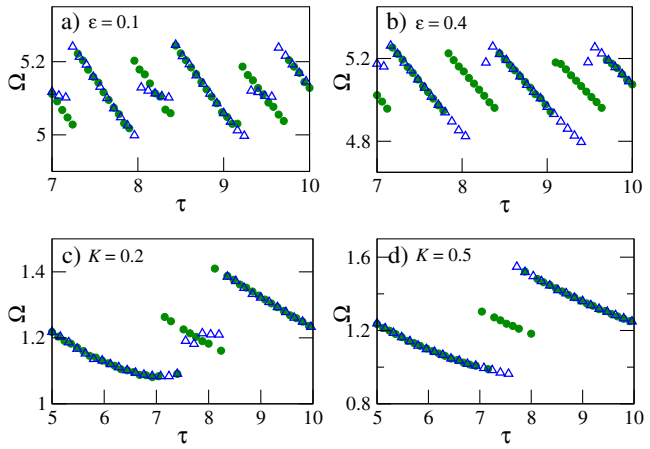


FIG. 7. Synchronized frequencies Ω as a function of delay τ for globally delay-coupled (*i*) Rössler oscillators (top row: (a) and (b)) and (*ii*) FitzHugh-Nagumo system (bottom row: (c) and (d)). Frequencies are plotted for the ensemble of $N=2$ (green circles) and $N=10$ (blue triangles) at two different coupling values.

For simulations, we fixed the parameters $a=0.2$, $f=0.2$, $c=10$, and the natural frequencies are all set to $\omega_i=5$. The effect of system size on synchronized frequencies at different coupling strengths are shown in Figs. 7(a) and 7(b), where we plot the variation of the synchronized frequency for the Rössler system as a function of delay $\tau$ for system sizes $N=2$ (green circles) and $N=10$ (blue triangles), and different coupling, $\varepsilon=0.1$ in (a) and $\varepsilon=0.4$ in (b). Comparing with similar results for the Landau-Stuart system in Fig. 3(b) show that in both cases, the in-phase frequencies of the system remain unaltered whereas mixed-phase frequencies are modified as a function of the system size $N$. Similarly, the mixed-phase frequencies disappear (Fig. 7(b)) in the Rössler system at higher coupling strengths as well.

Quantitatively similar results are obtained for delay coupled FitzHugh-Nagumo neuronal model systems, shown in Figs. 7(c) and 7(d). The equations of this model system are given by

$$\begin{aligned} \varepsilon\dot{u}_i &= u - \frac{1}{3}u_i^3 - v_i + \frac{K}{(N-1)}\sum_{j\neq i}\big(u_j(t-\tau) - u_i(t)\big), \\ \dot{v}_i &= u_i + a. \end{aligned} \tag{24}$$

We set the parameter values $a=\varepsilon=0.5$ and numerically analyze the frequency response of the system at different coupling strengths $K=0.2$ (Fig. 7(c)) and $K=0.5$ (Fig. 7(d)). Here, again the phase behavior of the system corresponding to in- and mixed-phase frequencies is very similar to the Rössler or the Landau–Stuart system: mixed-phase dynamics disappears for higher coupling strengths and larger system size as can be seen in Fig. 7(d).

## VI. SUMMARY AND DISCUSSION

In this work, we have considered the dynamics of a network of oscillators coupled globally and with time-delay. The system adopts distinct synchronized solutions: All the oscillators can be in-phase or the phases can be mixed. In this latter instance, the phases can be uniformly distributed on the circle, namely, the splay phase, or the phases can be arbitrary. For both situations, our numerical results are supported by analysis. Some solutions do not depend upon the delay parameter, while others occur only for certain values of the delay. We find that regardless of the size of the network, the frequency of oscillation can be calculated in a mean-field approximation, Eq. (11).

For appropriate values of coupling strength, small networks of oscillators show transitions between the in phase and mixed states when the time-delay is varied. However, for larger networks, we observe that the mixed phase vanishes, however leaving a vestige of the transition in a frequency jump that accompanies a transition between two in-phase solutions. This result generalizes the phase-flip transition which has been extensively studied for two oscillators.[19,20,30,31] The critical value of number of oscillators for which the mixed phase disappears depends exponentially on the coupling strength. Stability analysis for splay states confirms this observation.

Our results appear to hold for any system where the phase is properly defined: we numerically demonstrate this for globally coupled Rössler and Fitzhugh-Nagumo neuronal model. Furthermore, when the oscillators are mismatched,[39] there is a similar variation in $\tilde{c}$ with $N$ (cf. Fig. 3).

Thus, the present results make it possible to determine the phase dynamics for a specified number of oscillators and for a given coupling strength and also to estimate the synchronized frequency, Eq. (11) for a large number of oscillators, mainly for the mixed-phase solutions. In this case, $\tilde{c}\to 0$ as $N\to\infty$, and the synchronized frequency for large $N$ is approximately equal to the intrinsic frequencies from Eq. (11) and the oscillators are effectively uncoupled. Finally, it can also be surmised that the complexity, namely, the number of different phase configurations in the system, reduces as the size of the system grows.

## ACKNOWLEDGMENTS

We thank the Department of Science and Technology, India, for research support. R.R. is a recipient of the J. C. Bose fellowship of the DST.

[1]J. Buck and E. Buck, Science **159**, 1319 (1968).
[2]Z. Néda *et al.*, Nature (London) **403**, 849 (2000).
[3]Z. Jiang and M. McCall, J. Opt. Soc. Am. **10**, 155 (1993); K. Wiesenfeld, C. Bracikowski, G. James, and R. Roy, Phys. Rev. Lett. **65**, 1749 (1990).
[4]Y. Kuramoto, *Chemical Oscillations, Waves and Turbulence* (Springer-Verlag, Berlin, 1984).
[5]I. Z. Kiss, Y. Zhai, and J. L. Hudson, Science **296**, 1676 (2002).
[6]A. T. Winfree, *The Geometry of Biological Time* (Springer, New York, 1980).
[7]S. H. Strogatz, Physica **143D**, 1 (2000).
[8]A. Pikovsky, M. Rosenblum, and J. Kurths, *Synchronization: A Universal Concept in Nonlinear Sciences* (Cambridge University Press, Cambridge, 2001).
[9]S. H. Strogatz, *Sync: The emerging Science of Spontaneous Order* (Hyperion, New York, 2003).
[10]M. Lakshmanan and D. V. Senthilkumar, *Dynamics of Nonlinear Time-Delay Systems* (Springer-Verlag Berlin, 2011); F. M. Atay, *Complex Time-Delay Systems* (Springer-Verlag, Berlin, 2010); K. Gopalsamy, *Stability and Oscillations in Delay Differential Equations of Population Dynamics* (Kluwer Academic Publishers, Dordrecht, The Netherlands, 1992).
[11]N. MacDonald, *Time Lags in Biological Models*, Lect. Notes in Biomath. Vol. 27 (Springer, Berlin, 1978); J. M. Cushing, *Integrodifferential*

*Equations and Delay Models in Population Dynamics*, Lect. Notes in Biomath. Vol. 20 (Springer–Verlag, New York, 1977); "Delayed complex systems," edited by W. Just, A. Pelster, M. Schanz, and E. Schöll, Theme issue of Phil. Trans. R. Soc. A **368**, 303 (2010).
[12]D. V. R. Reddy, A. Sen, and G. L. Johnston, Phys. Rev. Lett. **80**, 5109 (1998); F. M. Atay, Phys. Rev. Lett. **91**, 094101 (2003); I. Fischer *et al*., Phys. Rev. Lett. **97**, 123902 (2006); G. Saxena, A. Prasad, and R. Ramaswamy, Phys. Rev. E **82**, 017201 (2010).
[13]H. G. Schuster and P. Wagner, Prog. Theor. Phys. **81**, 939 (1989).
[14]S. Yanchuk, Phys. Rev. E **72**, 036205 (2005); S. Yanchuk and P. Perlikowski, Phys. Rev. E **79**, 046221 (2009).
[15]M. J. Bünner and W. Just, Phys. Rev. E **58**, 4072 (1998).
[16]M. K. S. Yeung and S. H. Strogatz, Phys. Rev. Lett. **82**, 648 (1999); M. G. Earl and S. H. Strogatz, Phys. Rev. E **67**, 036204 (2003); V. Flunkert, S. Yanchuk, T. Dahms, and E. Schöll, Phys. Rev. Lett. **105**, 254101 (2010).
[17]A. Prasad, Phys. Rev. E **72**, 056204 (2005); R. Karnatak, R. Ramaswamy, and A. Prasad, Phys. Rev. E **76**, 035201 (2007); A. Prasad, M. Dhamala, B. M. Adhikari, and R. Ramaswamy, Phys. Rev. E **82**, 027201 (2010).
[18]G. Saxena, A. Prasad, and R. Ramaswamy, Phys. Rep. **521**, 205 (2012); G. Saxena, N. Punetha, A. Prasad, and R. Ramaswamy, AIP Conf. Proc. **1582**, 158 (2014).
[19]A. Prasad, J. Kurths, S. K. Dana, and R. Ramaswamy, Phys. Rev. E **74**, 035204 (2006); A. Prasad *et al*., Chaos **18**, 023111 (2008).
[20]C. Masoller, M. C. Torrent, and J. Garcia-Ojalvo, Phil. Trans. R. Soc. A **367**, 3255 (2009); J. M. Cruz, J. Escalona, P. Parmananda, R. Karnatak, A. Prasad, and R. Ramaswamy, Phys. Rev. E **81**, 046213 (2010); A. Sharma, M. D. Shrimali, A. Prasad, R. Ramaswamy, and U. Feudel, Phys. Rev. E **84**, 016226 (2011).
[21]P. Hadley and M. R. Beasley, Appl. Phys. Lett. **50**, 621 (1987).
[22]S. Nichols and K. Wiesenfeld, Phys. Rev. A **45**, 8430 (1992); S. H. Strogatz and R. E. Mirollo, Phys. Rev. E **47**, 220 (1993); R. Zillmer, R. Livi, A. Politi, and A. Torcini, Phys. Rev. E **76**, 046102 (2007).
[23]C. U. Choe, T. Dahms, P. Hövel, and E. Schöll, Phys. Rev. E **81**, 025205 (2010).
[24]K. Blaha, J. Lehnert, A. Keane, T. Dahms, P. Hövel, E. Schöll, and J. L. Hudson, Phys. Rev. E **88**, 062915 (2013).
[25]C. R. S. Williams, F. Sorrentino, T. E. Murphy, and R. Roy, Chaos **23**, 043117 (2013).
[26]Mixed-phase solutions are configurations that are not synchronized in-phase. The splay-phase, where phases are equally spaced, is one such solution, the occurrence of which does not depend on parameter values, but other mixed-phase solutions with irregularly distributed phases depend upon coupling parameters.
[27]B. M. Adhikari, A. Prasad, and M. Dhamala, Chaos **21**, 023116 (2011).
[28]W. Singer, Neuron **24**, 49 (1999); P. A. Tass *et al*., Phys. Rev. Lett. **81**, 3291 (1998).
[29]R. Vardi, A. Wallach, E. Kopelowitz, M. Abeles, S. Marom, and I. Kanter, Europhys. Lett. **97**, 66002 (2012).
[30]R. Karnatak, N. Punetha, A. Prasad, and R. Ramaswamy, Phys. Rev. E **82**, 046219 (2010).
[31]N. Punetha, R. Karnatak, A. Prasad, J. Kurths, and R. Ramaswamy, Phys. Rev. E **85**, 046204 (2012).
[32]Eq. (1) is solved using fourth order Range–Kutta method. For different initial conditions, all quantities are measured in the synchronized regime after removing appropriate number of transients, i.e., when the system settles into a synchronized frequency $\Omega$. In amplitude death region, this frequency is that of the damped motion. For Lyapunov exponents calculation, see J. D. Farmer, Physica **4D**, 366 (1982); we use integration step $\tau/700$.
[33]For the mixed phases, we found that the numerator in Eq. (10) varies linearly with number of oscillators and hence $\tilde{c}$ varies as $-1/(N-1)$.
[34]When the size (dimension) of a coupled system is increased, it exhibits very complex behaviors which generally are not observed in low dimensions. Examples are multistability, amplitude death, riddling, etc. Here, for certain coupling values, we observe that mixed-phases disappear with increasing network size. Therefore, the system simply goes to in-phase state. The complexity in phase behavior is thus reduced in higher dimensions.
[35]L. M. Pecora and T. L. Carroll, Phys. Rev. Lett. **80**, 2109 (1998).
[36]M. Dhamala, V. K. Jirsa, and M. Ding, Phys. Rev. Lett. **92**, 074104 (2004).
[37]W. Kinzel, A. Englert, G. Reents, M. Zigzag, and I. Kanter, Phys. Rev. E **79**, 056207 (2009).
[38]Except when $N=2$, for splay (anti-phase) solutions, $\alpha_{21}=-\alpha_{12}=\pi$. The coefficients for this specific case, $\cos(-\Omega\tau+\pi)=\cos(-\Omega\tau-\pi)=-\cos(\Omega\tau)$ do not depend upon $i$, $j$. However, this simplification does not apply for arbitrary $N$.
[39]Similar results are seen for ensembles of globally coupled non-identical oscillators, where the internal frequencies $\omega$'s in Eq. (1), are drawn from a Gaussian distribution with the same mean and different variances.